

Mechanism of Lateral Movement of Filopodia and Radial Actin Bundles across Neuronal Growth Cones

R. Oldenbourg, K. Katoh, and G. Danuser

Marine Biological Laboratory, Woods Hole, Massachusetts 02543 USA

ABSTRACT We investigated the motion of filopodia and actin bundles in lamellipodia of motile cells, using time-lapse sequences of polarized light images. We measured the velocity of retrograde flow of the actin network and the lateral motion of filopodia and actin bundles of the lamellipodium. Upon noting that laterally moving filopodia and actin bundles are always tilted with respect to the direction of retrograde flow, we propose a simple geometric model for the mechanism of lateral motion. The model establishes a relationship between the speed of lateral motion of actin bundles, their tilt angle with respect to the direction of retrograde flow, and the speed of retrograde flow in the lamellipodium. Our experimental results verify the quantitative predictions of the model. Furthermore, our observations support the hypothesis that lateral movement of filopodia is caused by retrograde flow of tilted actin bundles and by their growth through actin polymerization at the tip of the bundles inside the filopodia. Therefore we conclude that the lateral motion of tilted filopodia and actin bundles does not require a separate motile mechanism but is the result of retrograde flow and the assembly of actin filaments and bundles near the leading edge of the lamellipodium.

INTRODUCTION

Motile cells such as fibroblasts, keratocytes, epithelial cells, and neuronal growth cones, that crawl on natural or artificial substrates, require for their translocation the formation of a thin, peripheral sheet of cytoplasm, called the lamellipodium. The lamellipodium projects in the direction of cell advance; its functions include the establishment of initial adhesion points between the cell and the substrate, the recognition of target signals, and the control of cell advance (Abercrombie, 1980).

The leading edge of the lamellipodium often shows spike-like protrusions, called filopodia, that elongate, retract, and move laterally along the edge. The core of each filopodium is formed by a bundle of actin filaments that extends into the lamellipodium (Yamada et al., 1970, 1971; Tosney and Wessells, 1983; Lewis and Bridgman, 1992). The motile activities of filopodia and of the actin cytoskeleton in the lamellipodium have been investigated extensively by various light microscopic techniques (Soranno and Bell, 1982; Bray and Chapman, 1985; Wang, 1985; Goldberg and Burmeister, 1986; Forscher and Smith, 1988; Theriot and Mitchison, 1991; Welnhöfer et al., 1997; Katoh et al., 1999b). Many of these studies focused on the molecular mechanisms of lamellipodial protrusion in the direction of cell advance and of retrograde flow of cytoplasmic ma-

terial that was observed to move away from the leading edge to the back of the lamellipodium. However, the mechanism by which the filopodia and the associated actin filament bundles are translated laterally across the leading edge of the lamellipodium has remained a mystery until now (Mitchison and Cramer, 1996).

Victor Small (Small, 1994) first pointed out a simple mechanism for the lateral flow of actin filaments near the leading edge. The mechanism is based on a geometric argument that involves a cross-woven carpet of actin filaments and its continuous assembly by actin polymerization near the leading edge. In this model the carpet network, once formed, remains stationary with respect to the substrate, as is commonly observed in keratocytes. The lateral motion only occurs at the leading edge because of the addition of actin subunits to the ends of tilted filaments. Fig. 1 is taken from Small's publication and illustrates the model that predicts lateral movement of filament ends along the leading edge by extending a stationary actin network.

In this paper we propose a model for the lateral movement of f-actin-based structures that undergo retrograde flow in the lamellipodium. We analyze the lateral motion of filopodia and actin bundles in lamellipodia of slowly advancing growth cones. Our analysis is based on time-lapse movies of polarized light images recorded from unstained, living growth cones of *Aplysia* bag cell neurons (Katoh et al., 1999b). Specifically, we examine the relationship between the orientation of actin bundles, their lateral motion, and the speed and direction of retrograde flow of the actin network. The analysis of our experiments supports the conclusion that the lateral motion of filopodia and actin bundles near the leading edge in growth cones of *Aplysia* bag cell neurons does not require an independent motile mechanism. Instead, we propose that filopodia and their associated actin bundles are translated laterally across the leading edge only if they are tilted with respect to the retrograde flow direc-

Received for publication 19 July 1999 and in final form 19 November 1999.

Address reprint requests to Dr. Rudolf Oldenbourg, Marine Biological Laboratory, Woods Hole, MA 02543. Tel.: 508-289-7426; Fax: 508-540-6902; E-mail: rudolfo@mbi.edu.

Dr. Katoh's present address is Supermolecular Division, Electrotechnical Laboratory, 1-1-4 Umezono, Tsukuba, Ibaraki 305-8568, Japan.

Dr. Danuser's present address is Laboratory for Biomechanics, Swiss Federal Institute of Technology, Wagistrasse 4, CH-8952 Schlieren, Switzerland.

© 2000 by the Biophysical Society

0006-3495/00/03/1176/07 \$2.00

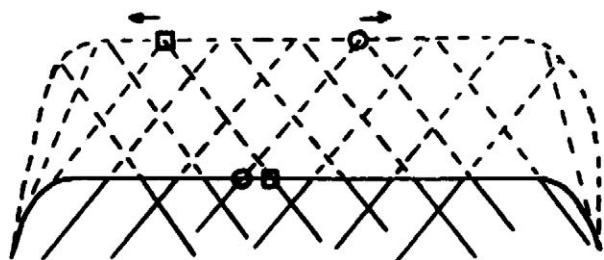


FIGURE 1 Schematic illustrating lamellipodium protrusion based on the polymerization of diagonally arranged actin filaments. The protrusion is associated with a lateral movement of filament ends (circle and square) along the cell membrane (reproduced from Small, 1994).

tion. Furthermore, the lateral motion of tilted filopodia and bundles is driven by the combination of retrograde flow of the actin network and its continuous extension by actin polymerization near the leading edge.

We also point out that the widely accepted model of a “carpet” of cross-woven actin filaments that is moved rearward by retrograde flow and extended by actin polymerization near the leading edge inherently predicts that the polymerization rate at the tip of actin filaments has to vary with their tilt angle. While filaments are transported away from the leading edge, the filament tips are elongated and remain near the edge. This means that for actin bundles that are tilted with respect to retrograde flow, the rate of elongation has to increase with the tilt angle. This prediction also applies to filopodia that move across the lamellipodium. Further experiments are necessary to corroborate this prediction, which seems to represent an important prerequisite for models that describe molecular mechanisms of actin polymerization near the leading edge of motile cells.

MATERIALS AND METHODS

Aplysia bag cell culture

Aplysia bag cell cultures were prepared in the BioCurrent Research Center at the Marine Biological Laboratory. Primary cell cultures of *Aplysia* bag cell neurons (Kaczmarek et al., 1979; Knox et al., 1992) were cultured on a coverslip bathed in artificial seawater. Growth cones were observed 1 or 2 days after the primary cell culture was started. For observation, the coverslips were mounted on glass slides with thin spacers (150 μm) and sealed to prevent evaporation. All observations were made at room temperature and within 4 h after we sealed the preparation.

Birefringence imaging

To directly and noninvasively observe actin bundles in living unstained growth cones, we imaged their birefringence, using a new type of polarized light microscope (Oldenbourg and Mei, 1995; Oldenbourg, 1996). The new Pol-Scope achieves high sensitivity and high resolution in its birefringence measurements by enhancing the traditional polarizing microscope with electrooptical devices, electronic imaging, and digital image processing. The Pol-Scope provides images whose brightness for each pixel is strictly

proportional to the birefringence retardation of the particular object point and independent of its slow axis orientation. Thus, unlike conventional polarizing microscopes, it provides a calculated birefringence distribution map that has no blind direction, regardless of the orientation of the molecular or fine-structural axis in the image plane.

The Pol-Scope measures the optical anisotropy as birefringence retardation (also called retardance; birefringence \times thickness). To gain a clear picture of the meaning of retardance we consider a light wave that passes through a birefringent sample of a certain thickness. In the birefringent material the light wave is separated into two orthogonally polarized waves, the o-ray and the e-ray, that travel at different speeds through the sample. Therefore, after traversing the sample, the wave fronts of the e-ray and o-ray are separated by a finite distance along the propagation direction of the light. This distance is called retardance, and it is measured as a length in nm (Hecht, 1998). The Pol-Scope measures the retardance in every resolved sample area simultaneously. The measured retardance maps are presented as images that show retardance values in shades of gray.

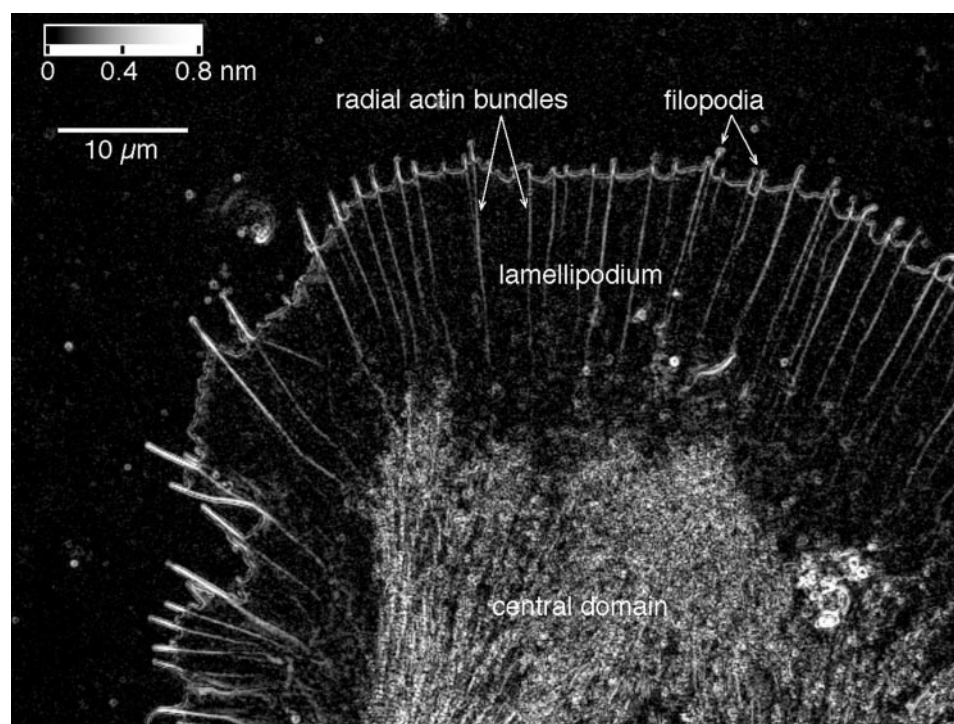
Fig. 2 is a Pol-Scope image of an unstained living growth cone with a large peripheral domain (called a lamellipodium) and a highly birefringent central domain that connects to the neurite. Recently we published a detailed account of the birefringent structures in growth cones of *Aplysia* bag cell neurons (Katoh et al., 1999b). According to this study, birefringence in the lamellipodium is mostly actin based, including the radial actin bundles that end in filopodia at the leading edge. The retardance of actin bundles is proportional to the number of filaments in the bundles (Katoh et al., 1996; Oldenbourg et al., 1998). The network of actin filaments that span the space between the radial bundles is generally not visible, indicating that the network exhibits little preferential alignment of the filaments. The front edge of the lamellipodium is seen as a birefringent double layer that is mainly caused by an optical effect called edge birefringence (Oldenbourg, 1991; Katoh et al., 1999b).

The microscope set-up used for the Pol-Scope measurements is described in more detail by Oldenbourg et al. (1998). The following is a list of instrument parts and settings employed in this study. We used a Nikon Microphot SA microscope equipped with an Apochromat, oil immersion condenser lens with aperture diaphragm (max. NA 1.4, typically set to 1.0 to improve sensitivity) and a 60 \times /1.4 NA Plan Apochromat objective lens, both selected for high extinction between crossed polarizers (all from Nikon, Melville, NY); a mercury arc lamp followed by an Ellis light scrambler (Technical Video, Woods Hole, MA) to homogeneously illuminate the back aperture of the condenser; and a narrow band pass interference filter ($\lambda = 546$ nm, 10 nm FWHM; Omega, Brattleboro, VT) to select the green mercury line for monochromatic illumination. Thus the optical resolution of the microscope was 0.23 μm , which was calculated using $\lambda/(\text{NA}_{\text{objective}} + \text{NA}_{\text{condenser}})$ (Inoué and Oldenbourg, 1995). The video rate CCD camera (C72; Dage/MTI, Michigan City, IN) recorded images with square pixels and a pixel-to-pixel distance of 0.115 μm measured in object space. The full image size was 640 \times 480 pixels.

For image acquisition, processing, and analysis we used a public-domain digital imaging platform (National Institutes of Health (NIH)-Image, developed at the U.S. National Institutes of Health and available on the Internet at <http://rsb.info.nih.gov/NIH-Image>), which was supplemented by custom-written software functions. To record time-lapse movies, sets of four raw images were recorded at regular time intervals over time spans of 15–30 min. Based on these images, Pol-Scope retardance magnitude maps were computed and assembled into image stacks for analysis of the dynamic behavior of living cells.

We recorded more than 100 time-lapse movies of living growth cones of *Aplysia* bag cell neurons. We selected one typical movie for the detailed analysis of the lateral motion of filopodia and actin bundles. The movie contains 181 frames, which were recorded at 5-s time intervals over 15 min. The time-lapse record was published as a QuickTime movie in an earlier publication (Movie 1; Katoh et al., 1999b).

FIGURE 2 Birefringent fine structure in the living growth cone of *Aplysia* bag cell neuron. This Pol-Scope image shows the peripheral lamellar domain containing radial actin bundles, which end in filopodia at the leading edge of the growth cone. Near the bottom is the central domain, which is filled with vesicles and highly birefringent fibers. The image is one frame of a time-lapse record that reveals the architectural dynamics of the cytoskeleton, including the formation of new filopodia and radial fibers and the continuous retrograde flow of birefringent elements in the peripheral domain. The gray wedge in the top left corner indicates the scale conversion from measured birefringence retardation to gray values.



RESULTS

Fig. 3 illustrates the motile behavior of a laterally traveling filopodium and actin bundle in the growth cone of an *Aplysia* bag cell neuron, in addition to showing nonmoving filopodia and radial actin bundles. In the image sequence one can also recognize the rearward motion of f-actin-based structural features, such as the crossing point of two bundles in the lamellipodium. As shown in previous publications (Katoh et al., 1999a,b), this rearward motion reveals the direction and speed of retrograde flow in the lamellipodium.

We measured the speed and direction of retrograde flow in several regions of a growth cone, using a time-lapse sequence of Pol-Scope images that was published earlier (Katoh et al., 1999b). We first identified a distinct structural feature, such as an intersection of two bundles, and then followed its path through the lamellipodium from one frame to the next. To measure the traveled distance accurately, we created a template that had the approximate shape of the structural feature and could be moved as an overlay across the image. We matched by eye the position of the template with the position of the structural feature in each frame and recorded the incremental displacements.

To reduce measurement errors we typically enlarged the region of interest fourfold. In the enlarged and digitally smoothed region, the position of the feature could be followed at a resolution of about one image pixel of the original recording or 115 nm in object space. To determine the speed of retrograde movement, we added position increments of five consecutive frames and divided by the elapsed time (25 s). For a given structural feature, we

obtained three to six sets of measurements along its path from the leading edge to near the central domain where actin filaments are disassembled.

The speed of retrograde flow determined by this method was remarkably stable in a given growth cone. The measured average value of $2.6 (\pm 0.25) \mu\text{m}/\text{min}$ (temperature $\approx 20^\circ\text{C}$) for the growth cone in Fig. 2 varied little between different regions in the lamellipodium and over a time period of 15 min.

Presumably, all f-actin-based structures in the lamellipodium undergo retrograde flow, including radial actin bundles. If radial bundles participate in retrograde flow, then their discernible motion should be affected by this continuous translation in the rearward direction. For example, a bundle that is tilted with respect to the direction of retrograde flow must exhibit an apparent lateral motion, i.e., a motion that is perpendicular to its bundle axis (Fig. 4). Furthermore, the speed of the apparent lateral motion must increase with increasing tilt angle of the bundle.

Therefore, based on the geometric relationship illustrated in Fig. 4, we speculate that the speed of retrograde flow, $|v_{\text{retro}}|$, the speed of lateral motion, $|v_{\text{lateral}}|$, and the tilt angle α of an actin bundle are related by the following expression:

$$|v_{\text{lateral}}| = |v_{\text{retro}}| \cdot \sin \alpha \quad (1)$$

To verify this relationship we measured the lateral velocity and the tilt angle of actin bundles in regions of a lamellipodium for which we independently determined the speed and direction of retrograde flow. Fig. 5 shows a laterally moving actin bundle and illustrates the procedure by which

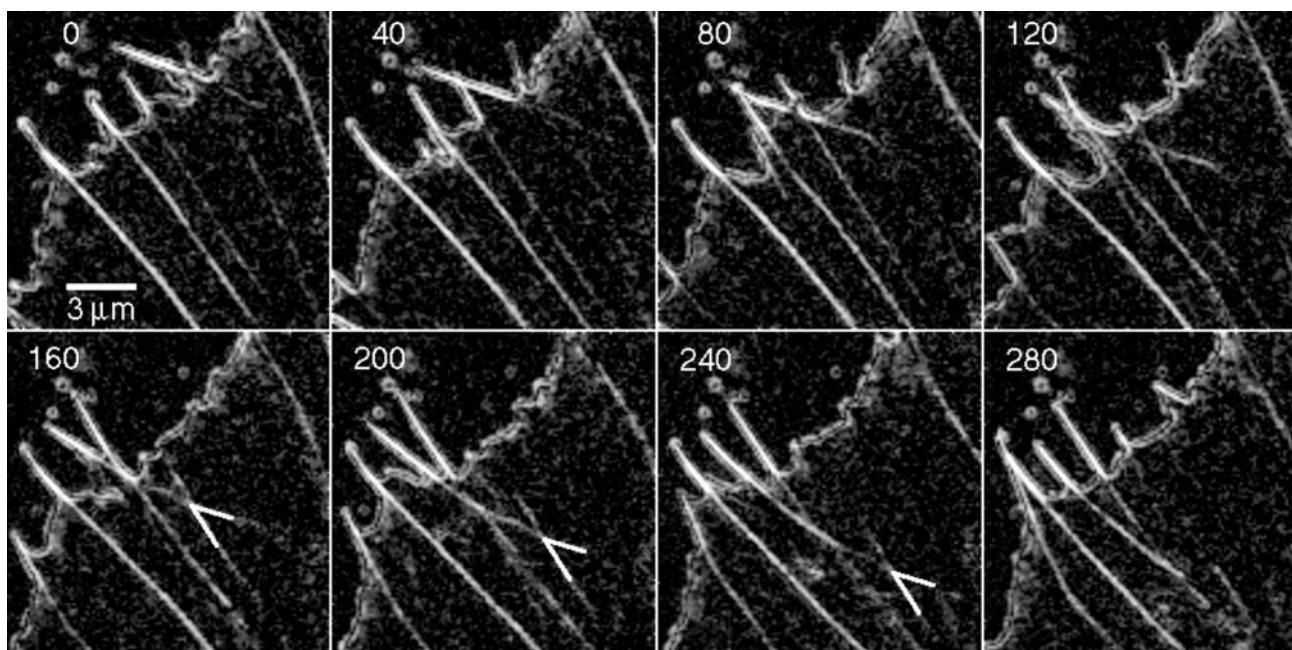


FIGURE 3 Image sequence showing filopodia at the leading edge and actin bundles in the lamellipodium of a neuronal growth cone. Most bundles and filopodia are roughly parallel to each other. One filopodium and bundle, however, is tilted and travels laterally. Numbers in the upper left corner indicate the time in seconds. At time points 160, 200, and 240 the tip of a triangular template shows the crossing point of two bundles. The displacement of the tip between consecutive frames was used to measure the speed of retrograde flow. (Enlarged and digitally smoothed image portions were taken from a time-lapse sequence that was published as Movie 1 in Katoh et al. (1999b).)

we measured its lateral displacements. The speed of lateral motion was calculated as the lateral displacement divided by the elapsed time.

The direction and speed of retrograde flow in the vicinity of a tilted bundle were determined independently either by observing a specific structural feature associated with the tilted bundle itself or by interpolating values for speed and direction of retrograde flow that were measured in the surroundings of the tilted bundle.

Tilted bundles frequently intersect other radially aligned bundles. As demonstrated above, the point of intersection can be used to measure the speed and direction of retrograde flow. This method gave the most reliable values for measuring retrograde flow in the vicinity of a tilted bundle.

If the tilted bundle itself did not exhibit an intersection with other radial bundles, the direction and speed of retrograde flow was determined at several points in the surrounding of the tilted bundle. Subsequently, those values of speed and direction of retrograde flow were interpolated to the region where the lateral speed of the tilted bundle was measured.

Fig. 6 summarizes the experimental results of lateral speed measurements on three tilted bundles. To be able to compare measurements of tilted bundles that move in regions that exhibited different speeds of retrograde flow, we plotted the ratio of lateral speed to retrograde flow versus the tilt angle α . The continuous line in Fig. 6 represents the expected sine relationship based on Eq. 1. The good agree-

ment between measured and predicted values confirms the validity of our geometric model, which describes the relationship between lateral and retrograde movement of tilted bundles.

Our movie records show that the movement of filopodia near the front edge is closely related to the movement of their associated actin bundles. A filopodium that travels laterally is associated with a tilted actin bundle. The larger the tilt angle is, the faster is the lateral movement of the actin bundle and its filopodium. To describe the movement of a filopodium and its actin bundle, we need to consider both actin polymerization near the leading edge and the retrograde flow of f-actin inside the lamellipodium. In the Discussion we will examine the hypothesis that these two mechanisms together produce the lateral motion of filopodia across the leading edge of a growth cone.

DISCUSSION

We are presenting a model of lateral motion of filopodia and actin bundles in growth cones of *Aplysia* bag cell neurons. The model is based on two independent motile mechanisms that have been proposed before as the two main engines behind the advance and retraction of lamellipodia: the retrograde flow of f-actin in the lamellipodium and the polymerization of f-actin near the leading edge. We propose that the observed lateral movement of filopodia and actin bun-

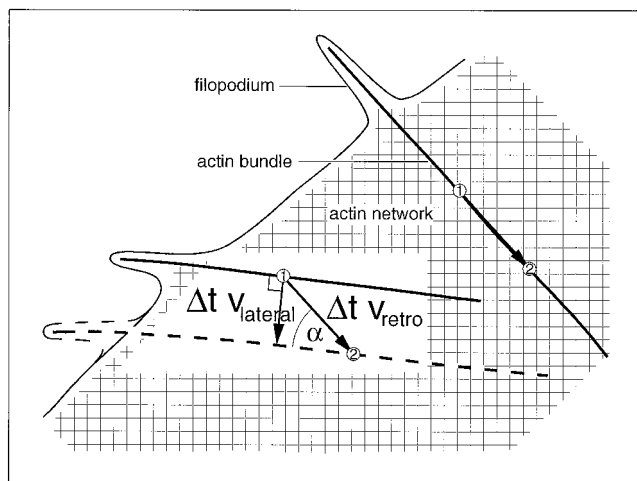


FIGURE 4 Geometric model illustrating the proposed relationship between lateral motion of a tilted actin bundle and retrograde flow of all actin-based structures in the lamellipodium. The movement of the bundles is illustrated by their displacements between two time points 1 and 2. Points labeled 1 and 2 that are connected by a vector represent the positions of the same structural element at the two time points. The position of the tilted bundle has visibly changed because of its lateral displacement. The lateral displacement is shown as $\Delta t v_{\text{lateral}}$, where v_{lateral} is the vector of the velocity perpendicular to the bundle axis and $\Delta t = t_2 - t_1$ is the elapsed time. The directed movement of the bundle, however, is not parallel to v_{lateral} , but is in the direction of retrograde flow, indicated by the vector v_{retro} . $\Delta t v_{\text{retro}}$ represents the displacement of a physical bundle element between time points 1 and 2. The lateral movement of the bundle is proportional to its tilt angle α . If a bundle is not tilted with respect to retrograde flow, like the bundle on the right side, the bundle and its associated filopodium do not exhibit lateral motion and are called stationary. Notice that in this case a physical bundle element is moving along the bundle axis. Unless the element represents a structural feature this movement is not discernible.

dles can be fully explained on the basis of these two mechanisms alone.

In testing our hypothesis we measured the speed and direction of retrograde flow, using the progression of structural features such as the crossing point of two actin bundles in the lamellipodium. The measured speed of $2.6 \mu\text{m}/\text{min}$ for retrograde flow is close to the value measured using artificial markers in fluorescence or differential interference contrast microscopy (Lin and Forscher, 1995).

In addition to retrograde flow, actin assembly near the leading edge plays a critical role in shaping the front edge of an advancing growth cone. The poisoning of actin assembly by cytochalasins, for example, has catastrophic effects on the maintenance of the actin network in the lamellipodium. With the exposure of *Aplysia* growth cones to cytochalasin B, all f-actin structures are removed from the lamellipodium (Forscher and Smith, 1988). The retraction of the actin network, which takes with it much of the cytoplasm, starts at the leading edge and progresses toward the base of the lamellipodium with the speed of retrograde flow.

Therefore, it was proposed that a dynamic equilibrium between retrograde flow and actin polymerization controls

the movement of the front edge of a growth cone (Lin et al., 1996). To maintain a steady state the polymerization rate at the front edge is equal to the retrograde flow rate, while for cell advance the polymerization rate is larger than retrograde flow and vice versa for lamellipodial retraction. We note, however, that the polymerization rate for individual filament ends depends on their orientation. To maintain a steady front edge, for example, filaments that are tilted with respect to the retrograde flow direction have to polymerize at a higher rate than filaments that are parallel to retrograde flow. We will return to this issue below.

The hypothesis of an actin network that is assembled at the leading edge and is moved with relatively little distortion to the back of the lamellipodium was supported by our recent results from a kymographic analysis of time-lapsed polarized light images of lamellipodia of neuronal growth cones (Katoh et al., 1999a).

Our analysis is based on observations of growth cones that were advancing at a rate of less than $1 \mu\text{m}/\text{min}$. For simplicity's sake, our discussion of observed filopodia and actin bundle motion will assume a steady-state front edge, where, on average, retrograde flow of f-actin structures is balanced by their assembly near the leading edge.

The extension and retraction of filopodia and their associated actin bundles seem to be based on the same interplay of actin assembly and retrograde flow (Lin et al., 1996; Katoh et al., 1999b). Increased assembly rates near the tip of an actin bundle push its filopodium forward, while decreased assembly rates in combination with the rearward pull of the bundle, which is anchored in the actin network of the lamellipodium, lead to the retraction of the filopodium.

Our model of lateral motion of filopodia and actin bundles has some interesting consequences:

1. A radial actin bundle that maintains a stable position, on average, is oriented parallel to the direction of retrograde flow. Hence the axis of a stable bundle indicates the direction of retrograde flow. In an upcoming paper (Danuser and Oldenbourg, manuscript submitted for publication) we analyze the small fluctuations that occur around the stable position. As we show, the fluctuations can be exploited to measure the direction and speed of retrograde flow around a stable bundle.

2. As mentioned earlier, the polymerization rate at the tip of an actin filament or bundle varies with the angle α between the bundle and the direction of retrograde flow. To maintain the length of a laterally moving filopodium, like the one shown in Fig. 4, the polymerization rate at the tip of its actin bundle must be equal to $v_{\text{retro}}/\cos \alpha$ (the length of a filopodium is measured from its tip to its base, where the cell membrane detaches from the core of the filopodium). Hence, to maintain the length of a bundle that is tilted by $\alpha = 60^\circ$, for example, the polymerization rate is twice the rate of a bundle that is parallel to retrograde flow. For angles approaching 90° this can lead to unrealistically high poly-

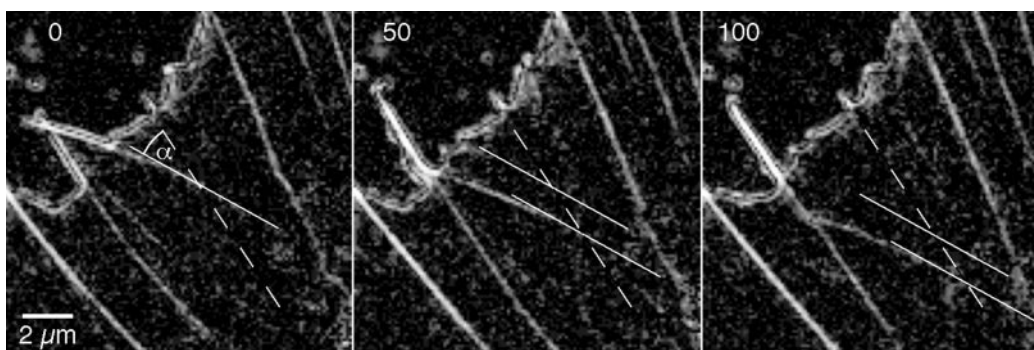


FIGURE 5 Image sequence showing traveling bundle and the analysis of its lateral motion. The left image shows a full line that was drawn as a tangent to the tilted bundle. In the center image that line is repeated, and in addition a parallel but shifted line is drawn tangent to the new position of the bundle. The shortest distance between the two lines (distance parallel to the normal of the lines) is equal to the lateral displacement of the bundle during the elapsed period (50 s). The right image illustrates the lateral travel between time points 50 and 100. The dashed line indicates the direction of retrograde flow, which was determined at a later time by the appearance of a stable bundle in this region of the lamellipodium (the filopodium associated with this radial bundle is already visible at the leading edge). In the left image, the tilt angle α is indicated. (Enlarged and digitally smoothed image portions were taken from a time-lapse sequence that was published as Movie 1 in Katoh et al. (1999b).)

merization rates, suppressing the occurrence of highly tilted filopodia and actin bundles.

3. So far we have considered lateral motion that is measured perpendicular to the long axis of a linear structure such as a filopodium or bundle. This is a natural choice, because any motion parallel to the axis of a linear structure is not discernible, unless there is a structural feature attached to the bundle, such as a sudden drop in the number

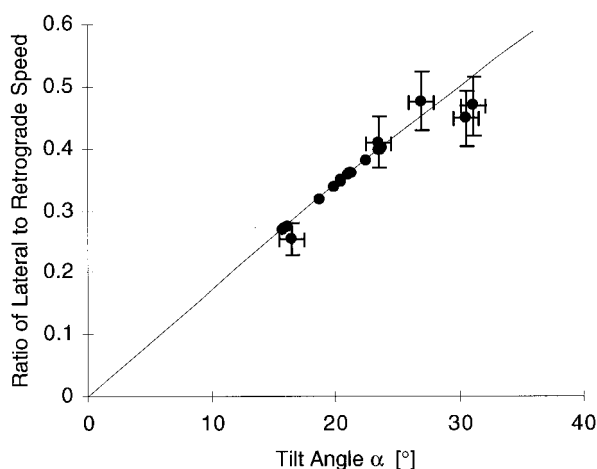


FIGURE 6 Graph of lateral speed of tilted bundles versus tilt angle. The lateral speed is expressed as a fraction of the independently measured retrograde flow speed. The graph shows measurements that were taken on three different actin bundles. A bundle was typically analyzed in segments, and the tilt angle with respect to the direction of retrograde flow was determined for each segment. Data points without error bars represent measurements on tilted bundles that intersected other radial bundles and thus provided markers to measure the speed and direction of retrograde flow in the direct vicinity of the tilted bundles. Data points with error bars were measured using interpolated values for speed and direction of retrograde flow. The continuous line shows the predicted sine relationship based on Eq. 1.

of filaments or a fork where one bundle splits into two. Near the front of a growth cone, however, the leading edge provides an alternative reference direction for measuring the speed of laterally moving filopodia. Note, however, that regardless of the direction we choose for measuring the lateral motion, our model proposes that the actual displacements of physical bundle segments only occur in the direction of and with the speed of retrograde flow (see Fig. 4).

When lateral motion parallel to the leading edge is measured, quite high lateral speeds can be found. If the leading edge extends perpendicular to retrograde flow, as is approximately the case, then a tilted filopodium travels parallel to the leading edge at a speed of $v_{\text{retro}} \tan \alpha$. For angles α larger than 45° this leads to speeds higher than v_{retro} . Our time-lapse movies show some highly tilted, short-lived filopodia that exceed v_{retro} in their motion parallel to the leading edge. Similar observations are reported by Fisher et al. (1988).

We have not yet addressed the question of why actin bundles are tilted. At this point we can only speculate and point to the location where one might be able to find at least part of the answer: the narrow zone of cytoplasm behind the leading edge, where most of the actin assembly seems to occur (Forscher and Smith, 1988). In this zone, which includes the cell membrane, existing actin filaments are extended and new ones are nucleated by yet unknown mechanisms that seem to provide for a distribution of filament orientations. Filopodia might form through the bundling of filaments and/or the concerted nucleation of many parallel filaments. What controls the initial orientation of new filaments and filopodia is not known, but our observations seem to indicate that a range of orientations does occur.

Existing bundles are extended mainly parallel to their axis in accordance with their mechanical stiffness. The

persistence length of a single actin filament in vitro is $\sim 18 \mu\text{m}$ (Gittes et al., 1993). The actin bundle at the core of a filopodium contains ~ 15 actin filaments or more (Katoh et al., 1999b), and its persistence length is proportionately higher. Hence we speculate that the growth of a filopodium occurs mainly in the direction of the actin bundle that forms the core of the filopodium. A significant reorientation of the growth direction might occur over distances that correspond to the persistence length of the bundle.

In conclusion, we have analyzed the lateral motion of filopodia and radial actin bundles in lamellipodia of growth cones of *Aplysia* bag cell neurons. Based on our observations we propose a model that attributes lateral motion of tilted filopodia and actin bundles to retrograde flow and the assembly of actin filaments and bundles near the leading edge. Our model has interesting consequences for the dynamics of actin assembly near the leading edge in general. We anticipate that the results of our analysis are transferable to other cell types that use a similar molecular machinery for their translocation.

We are grateful to Shinya Inoué for advice and a careful reading of the manuscript.

We acknowledge support from the Swiss National Science Foundation in the form of a Young Investigator Award (to GD) and from the BioCurrent Research Center at the Marine Biological Laboratory, which is supported by National Institutes of Health grant P41RR-01385. This work was funded by National Institutes of Health grant GM 49210 (to RO).

REFERENCES

- Abercrombie, M. 1980. The crawling movement of metazoan cells. *Proc. R. Soc. Lond. B.* 207:129–147.
- Bray, D., and K. Chapman. 1985. Analysis of microspike movements on the neuronal growth cone. *J. Neurosci.* 5:3204–3213.
- Fisher, G. W., P. A. Conrad, R. L. DeBiasio, and D. L. Taylor. 1988. Centripetal transport of cytoplasm, actin, and the cell surface in lamellipodia of fibroblasts. *Cell Motil. Cytoskel.* 11:235–247.
- Forscher, P., and S. J. Smith. 1988. Actions of cytochalasins on the organization of actin filaments and microtubules in a neuronal growth cone. *J. Cell Biol.* 107:1505–1516.
- Gittes, F., B. Mickey, J. Nettleton, and J. Howard. 1993. Flexural rigidity of microtubules and actin filaments measured from thermal fluctuations in shape. *J. Cell Biol.* 120:923–934.
- Goldberg, D. J., and D. W. Burmeister. 1986. Stages in axon formation: Observation of growth of *Aplysia* axons in culture using video-enhanced contrast-differential interference contrast microscopy. *J. Cell Biol.* 103:1921–1931.
- Hecht, E. 1998. Optics, 3rd Ed. Addison-Wesley, Reading, MA.
- Inoué, S., and R. Oldenbourg. 1995. Microscopes. In *Handbook of Optics*, 2nd Ed., Vol. 2. M. Bass, editor. McGraw-Hill, New York. 17.1–17.52.
- Kaczmarek, L. K., M. Finbow, J. P. Revel, and F. Strumwasser. 1979. The morphology and coupling of *Aplysia* bag cell within the abdominal ganglion and in cell culture. *J. Neurobiol.* 10:535–550.
- Katoh, K., K. Hammar, P. J. S. Smith, and R. Oldenbourg. 1999a. Arrangement of radial actin bundles in the growth cone of *Aplysia* bag cell neurons shows the immediate past history of filopodial behavior. *Proc. Natl. Acad. Sci. USA.* 96:7928–7931.
- Katoh, K., K. Hammar, P. J. S. Smith, and R. Oldenbourg. 1999b. Birefringence imaging directly reveals architectural dynamics of filamentous actin in living growth cones. *Mol. Biol. Cell.* 10:197–210.
- Katoh, K., K. Yamada, F. Oosawa, and R. Oldenbourg. 1996. Birefringence measurements of the actin bundle in acrosomal processes of *Limulus* sperm. *Biol. Bull.* 191:271–272.
- Knox, R. J., E. A. Quattrocki, J. A. Connor, and L. K. Kaczmarek. 1992. Recruitment of Ca^{2+} channels by protein kinase C during rapid formation of putative neuropeptide release sites in isolated *Aplysia* neurons. *Neuron.* 8:883–889.
- Lewis, A. K., and P. C. Bridgman. 1992. Nerve growth cone lamellipodia contain two populations of actin filaments that differ in organization and polarity. *J. Cell Biol.* 119:1219–1243.
- Lin, C.-H., E. M. Espreafico, M. S. Mooseker, and P. Forscher. 1996. Myosin drives retrograde f-actin flow in neural growth cone. *Neuron.* 16:769–782.
- Lin, C.-H., and P. Forscher. 1995. Growth cone advance is inversely proportional to retrograde f-actin flow. *Neuron.* 14:763–771.
- Mitchison, T. J., and L. P. Cramer. 1996. Actin-based cell motility and cell locomotion. *Cell.* 84:371–379.
- Oldenbourg, R. 1991. Analysis of edge birefringence. *Biophys. J.* 60:629–641.
- Oldenbourg, R. 1996. A new view on polarization microscopy. *Nature.* 381:811–812.
- Oldenbourg, R., and G. Mei. 1995. New polarized light microscope with precision universal compensator. *J. Microsc.* 180:140–147.
- Oldenbourg, R., E. D. Salmon, and P. T. Tran. 1998. Birefringence of single and bundled microtubules. *Biophys. J.* 74:645–654.
- Small, V. J. 1994. Lamellipodia architecture: actin filament turnover and the lateral flow of actin filaments during motility. *Semin. Cell Biol.* 5:157–163.
- Soranno, T., and E. Bell. 1982. Cytostructural dynamics of spreading and translocating cells. *J. Cell Biol.* 95:127–136.
- Theriot, J. A., and T. J. Mitchison. 1991. Actin filament dynamics in locomoting cells. *Nature.* 352:126–131.
- Tosney, K. W., and N. K. Wessells. 1983. Neuronal motility: the ultrastructure of veils and microspikes correlates with their motile activities. *J. Cell Sci.* 61:389–411.
- Wang, Y. L. 1985. Exchange of actin subunits at the leading edge of living fibroblasts: possible role of treadmilling. *J. Cell Biol.* 101:597–602.
- Welnhöfer, E. A., L. Zhao, and I. Cohan. 1997. Actin dynamics and organization during growth cone morphogenesis in *Helisoma* neurons. *Cell. Motil. Cytoskel.* 37:54–71.
- Yamada, K. M., B. S. Spooner, and N. K. Wessells. 1970. Axon growth: role of microfilaments and microtubules. *Proc. Natl. Acad. Sci. USA.* 66:1206–1212.
- Yamada, K. M., B. S. Spooner, and N. K. Wessells. 1971. Ultrastructure and function of growth cones and axons of cultured nerve cells. *J. Cell Biol.* 49:614–635.